

# Nonlinear Operator Learning Using Energy Minimization and MLPs

Mats G. Larson, Carl Lundholm, Anna Persson

## Abstract

We develop and evaluate a method for learning solution operators to nonlinear problems governed by partial differential equations. The approach is based on a finite element discretization and aims at representing the solution operator by an MLP that takes latent variables as input. The latent variables will typically correspond to parameters in a parametrization of input data such as boundary conditions, coefficients, and right-hand sides. The loss function is most often an energy functional and we formulate efficient parallelizable training algorithms based on assembling the energy locally on each element. For large problems, the learning process can be made more efficient by using only a small fraction of randomly chosen elements in the mesh in each iteration. The approach is evaluated on several relevant test cases, where learning the solution operator turns out to be beneficial compared to classical numerical methods.

## 1 Introduction

In recent years, there has been a lot of interest in using machine learning methods in applied mathematics and scientific computing. In this work, the focus is on methods that approximate the solution operator to parameterized partial differential equations (PDEs). We emphasize that the aim is *not* to learn the solution to a single PDE problem, but rather to a family of the same type of PDE problems, by learning the mapping from a parameter space into the solution space.

There are several approaches to learning solution operators or solutions to PDEs in the literature. These can be divided into two main branches; data-driven or physics-informed. The data-driven methods are based on (typically pre-computed) data, such as e.g. Neural operators [6], Fourier neural operators [7], DeepONets [8], and the random feature model [9]. The physics-informed methods typically penalize the network to satisfy a PDE or other physical laws by designing an appropriate loss function, e.g. the Deep-Ritz method [4] and Physics-informed neural networks (PINNs) [11]. These methods do not require any data in general. Typically, the focus of physics-informed approaches has not been on learning parameterized problems, but mainly the solution to a single PDE problem.

In this paper we develop a data-free physics-informed method for operator learning of parameterized PDEs. We construct a neural network that learns a family of solutions by utilizing a loss functions based on energy minimization that penalizes the network to satisfy the PDE. This means that the computationally costly step of generating training data is avoided. The energy minimization approach has earlier been considered in neural network contexts, e.g. [13] for finding low-dimensional models of physical motion and [12]

for applications in soft tissue modeling. In this work we generalize these approaches and develop a method that can be applied to any (nonlinear) problem with a given energy functional. The problem is first discretized using a finite element method (FEM) and a neural network is trained to learn the corresponding approximate solution operator. The input to the neural network is typically parameters to the problem which defines the data on e.g. the boundary, the coefficients, or the right-hand side. The output of the network is the finite element degrees of freedom (DOFs), which for standard P1 elements considered here are the function values at the nodes of the finite element mesh.

Furthermore, we provide a parallelized algorithm for computing the energy in each iteration, which is necessary for efficient training on GPUs. We also suggest to use random batches of elements in the mesh, which has potential to be useful in large problems with many degrees of freedom.

## 2 General setting and energy functionals

Consider a general nonlinear PDE which admits an energy functional  $E : V \rightarrow \mathbb{R}$  for a suitable space  $V$ . We are particularly interested in settings where the energy functional may depend on a parameter  $\mathbf{p} \in D \subseteq \mathbb{R}^d$ , typically through boundary conditions, coefficients, or right-hand sides. For a given set of parameters  $\mathbf{p}$ , the solution  $u \in V$  to the PDE is given by the minimization problem

$$u = \arg \min_{v \in V} E(v), \quad (2.1)$$

where we emphasize that  $E(v)$  depends on  $\mathbf{p}$ .

In this paper, we are interested in the solution operator to (2.1) depending on the parameter  $\mathbf{p}$ . Let  $\mathcal{A} : D \rightarrow V$  denote this solution operator such that  $u = \mathcal{A}(\mathbf{p})$ . Here  $\mathbf{p}$  is often referred to as the latent variable and  $D$  the latent space. Furthermore, we assume that the latent variable  $\mathbf{p}$  is a random variable with a given probability distribution  $\mathcal{P}$  over  $D$ .

### 2.1 Finite element discretization

To be able to learn the solution operator we first need to discretize  $V$ . For this purpose, we introduce a finite element discretization of the solution space  $V$ . Let  $\mathcal{T}_h$  denote a mesh based on a finite subdivision of  $\Omega$  into closed and convex elements of maximal diameter  $h$ , i.e.  $\text{diam}(T) \leq h$  for  $T \in \mathcal{T}_h$ . Let  $V_h \subseteq V$  be suitable finite element space based on the mesh  $\mathcal{T}_h$ . The corresponding approximation  $u_h \in V_h$  is attained by minimizing the energy functional over the finite element space  $V_h$

$$u_h = \arg \min_{v \in V_h} E(v). \quad (2.2)$$

We now define the discrete version of  $\mathcal{A}$ ,

$$\mathcal{A}_h : D \rightarrow V_h, \quad \text{such that} \quad u_h = \mathcal{A}_h(\mathbf{p}). \quad (2.3)$$

The aim is set up a neural network that approximates this mapping.

**Remark 2.1.** We emphasize that the definition of  $\mathcal{T}_h$  and  $V_h$  are intentionally very general. The numerical examples in Section 4 will be based on first order Lagrangian (P1) finite elements on triangles and tetrahedrons. However, in the current framework, it is possible to use many other types of elements and also higher order degree polynomials.

### 3 Operator learning with energy minimization

#### 3.1 Network architecture and loss function

We consider a simple feed-forward and fully connected network, often referred to as multilayer perceptron (MLP). The input layer is the latent variable  $\mathbf{p} \in D$  and the output layer is the nodal values of a finite element function in  $V_h$ . The size of the input layer is  $d$ , since  $\mathbf{p} \subseteq \mathbb{R}^d$ , and the size of the output layer equals the number of free nodes  $n$  in the mesh  $\mathcal{T}_h$ , i.e. nodes that do not correspond to a Dirichlet boundary condition.

The activation function mapping the hidden layers is set to the exponential linear unit (ELU) function

$$\sigma(x) = \begin{cases} x, & \text{if } x > 0, \\ e^x - 1, & \text{if } x \leq 0. \end{cases}$$

Let  $\theta$  denote the trainable weights in the network and let

$$\mathcal{A}_{h,\theta} : D \rightarrow V_h, \quad \text{such that} \quad u_{h,\theta} = \mathcal{A}_{h,\theta}(\mathbf{p})$$

describe the neural network approximation of  $\mathcal{A}_h$  in (2.3).

To train the network we use the the following loss functions which is based on the energy

$$\mathcal{L}(\theta) := \mathbb{E}_{\mathbf{p} \sim \mathcal{P}} [E(\mathcal{A}_{h,\theta}(\mathbf{p}))]. \quad (3.1)$$

The network thus learns the operator by minimizing the expected value of the energy with respect to the parameter  $\mathbf{p}$ . Since minimizing the energy (for a fixed  $\mathbf{p}$ ) is equivalent to solving the finite element problem, we expect the network to accurately approximate the (discretized) solution operator. This is further motivated in the next paragraph.

The method is based on the idea of learning the finite element approximation. This turns out to be beneficial when studying the error of the method. First we observe that during training, the loss function  $\mathcal{L}(\theta) = \mathbb{E}_{\mathbf{p} \sim \mathcal{P}} [E(\mathcal{A}_{h,\theta}(\mathbf{p}))]$  is indirectly minimized over a collection of functions in  $V_h$  and  $\mathbb{E}_{\mathbf{p} \sim \mathcal{P}} [E(\mathcal{A}_h(\mathbf{p}))]$  is the minimum over the set  $V_h$ . Hence, by assuming well-trainedness of the network we may assume that the error is small, i.e.

$$\mathbb{E}_{\mathbf{p} \sim \mathcal{P}} [E(\mathcal{A}_{h,\theta}(\mathbf{p})) - E(\mathcal{A}_h(\mathbf{p}))] \leq \epsilon,$$

for some  $\epsilon > 0$ . Second, the error between the finite element solution and the exact solution is typically known from the rich finite element theory. We shall combine both of these ideas to obtain an approximation error estimate in Theorem 3.1. To quantify the error we assume that the energy takes the form

$$E(v) = \frac{1}{2}(A\nabla v, \nabla v)_{L^2} - (f, v)_{L^2},$$

which is the case for a Poisson problem with coefficient  $A$  and right-hand side  $f$ , see the numerical examples in Section 4 for further details. We also assume that discretization is based on Lagrangian finite elements of order  $p$ . The error is measured in the following norm

$$\|v\|_a^2 := a(v, v) = (A\nabla v, \nabla v)_{L^2},$$

where we have the following identity.

**Lemma 3.1 (An energy identity).**

$$\frac{1}{2}\|u_h - v\|_a^2 = E(v) - E(u_h) \quad \forall v \in V_h$$

**Proof.** The right-hand side is

$$\begin{aligned} E(v) - E(u_h) &= \left( \frac{1}{2}\|v\|_a^2 - (f, v)_{L^2} \right) - \left( \frac{1}{2}\|u_h\|_a^2 - (f, u_h)_{L^2} \right) \\ &= \frac{1}{2}\|v\|_a^2 - \frac{1}{2}\|u_h\|_a^2 - \underbrace{(f, v - u_h)_{L^2}}_{\in V_h} \\ &= \frac{1}{2}\|v\|_a^2 - \frac{1}{2}\|u_h\|_a^2 - a(u_h, v - u_h) \\ &= \frac{1}{2}\|v\|_a^2 + \frac{1}{2}\|u_h\|_a^2 - a(u_h, v) \\ &= \frac{1}{2}\|u_h - v\|_a^2 \end{aligned}$$

■

Under these assumptions on the energy and the discretization we derive the following error bound.

**Theorem 3.1 (An energy estimate for the approximation error).** *There exists a positive constant such that*

$$\mathbb{E}_{\mathbf{p} \sim \mathcal{P}} [\|\mathcal{A}(\mathbf{p}) - \mathcal{A}_{h,\theta}(\mathbf{p})\|_a^2] \lesssim h^{2p} \left( \mathbb{E}_{\mathbf{p} \sim \mathcal{P}} [\|D^{p+1}\mathcal{A}(\mathbf{p})\|^2] \right) + \epsilon$$

**Proof.** Recall that  $u = \mathcal{A}(\mathbf{p})$  and  $u_{h,\theta} = \mathcal{A}_{h,\theta}(\mathbf{p})$ . Hence, the argument to the expectation operator on left-hand side is bounded by

$$\begin{aligned} \|u - u_{h,\theta}\|_a^2 &\lesssim \|u - u_h\|_a^2 + \|u_h - u_{h,\theta}\|_a^2 \\ &\lesssim h^{2p}\|D^{p+1}u\|^2 + E(u_{h,\theta}) - E(u_h) \end{aligned}$$

Here, we have started with an error split using  $\pm u_h$ , then applied a standard energy estimate for the finite element error and Lemma 3.1 for the learning error where we have used that  $u_{h,\theta} \in V_h$ . Taking the expected value of both sides preserves the inequality. Using linearity of the expected value and the well-trainedness assumption of the network gives the desired result. ■

### 3.2 Efficient learning

The network will be trained using an iterative method based on the stochastic gradient descent (SGD), e.g. the ADAM optimizer. To train the network efficiently, the computation of the gradient of the loss function in (3.1) needs to be fast. Typically, a mini-batch of instances is used to evaluate the expected value in (3.1). In each iteration of the optimization algorithm, a sample of size  $M$ , i.e.,  $\{\mathbf{p}_i\}_{i=1}^M$ , is generated from the distribution given by  $\mathcal{P}$ . The loss function in (3.1) is thus approximated by

$$\frac{1}{M} \sum_{i=1}^M E(\mathcal{A}_{h,\theta}(\mathbf{p}_i)). \quad (3.2)$$

We note that the energy in (3.2) requires a computation on each element in the mesh, i.e.

$$E(\mathcal{A}_{h,\theta}(\mathbf{p}_i)) = \sum_{T \in \mathcal{T}_h} E_T(\mathcal{A}_{h,\theta}(\mathbf{p}_i)),$$

where  $E_T$  denotes the local energy contribution on the element  $T$ . For, e.g., a Poisson problem,  $E_T$  would require the local assembly of the stiffness matrix and load vector. See section 4 for further examples in practice. We note that these computations can be made in parallel on e.g. a GPU. For large problems with many elements, we suggest to also use mini-batches for these elements. The mini-batch is based on a uniform selection of  $N$  elements  $\{T_i\}_{i=1}^N$  in each iteration, which is similar to the use of mini-batches in SGD. This means that the loss function is approximated by

$$\frac{1}{M} \sum_{i=1}^M \sum_{j=1}^N E_{T_j}(\mathcal{A}_{h,\theta}(\mathbf{p}_i)). \quad (3.3)$$

Note that we do not divide by  $N$ , since we do not aim to approximate an expected value but rather the integral over the full domain  $\Omega$ .

## 4 Examples

In this section we provide three examples to evaluate how the proposed method performs in practice. The first example considers a relatively simple parameterized PDE to introduce the energy minimization approach. The second example concerns a random PDE with a coefficient depending on a Gaussian random field. Gaussian random fields are of particular interest in, e.g., geophysical applications where the field can be used to describe porous media. The trained network can be used in uncertainty quantification, where the solution to the given PDE are needed many times for different realizations of the field. The third example concerns an application of solution operators for solving nonlinear elasticity problems.

The implementation used for the examples is based on the code presented in [13] which is publicly available at <https://github.com/nmwsharp/neural-physics-subspaces>. The training of the neural networks in the examples was enabled by resources provided by National Academic Infrastructure for Supercomputing in Sweden (NAISS) [1]. More precisely, the training has been performed on NVIDIA Tesla A100 HGX GPUs on the Alvis cluster.

### 4.1 A parameterized PDE

Consider the following parameterized Poisson problem

$$-\nabla(A(\mathbf{p}) \cdot \nabla u) = f, \quad \text{in } \Omega, \quad (4.1)$$

$$u = 0, \quad \text{on } \partial\Omega, \quad (4.2)$$

with  $\mathbf{p} = (x_0, y_0, r)$ ,  $f = 1$ , and

$$A(\mathbf{p}, x, y) = A(x_0, y_0, r, x, y) = 0.1 + \exp(-((x - x_0)^2 + (y - y_0)^2)/r).$$

This is a coefficient which is equal to 0.1 everywhere, except for a spike given by the exponential term. The parameters  $\mathbf{p} = (x_0, y_0, r)$  determine the location and the radius of the spike. In this example we consider  $\Omega = [-1, 1] \times [-1, 1]$ , a uniform distribution for the coordinates  $x_0, y_0 \sim U([-1, 1])$  (independent), and another uniform distribution for the radius  $r \sim U([0.01, 0.2])$ .

The weak form of (4.1)-(4.2) is given by the following; find  $u \in H_0^1$  such that

$$(A(\mathbf{p})\nabla u, \nabla v)_{L^2} = (f, v)_{L^2}, \quad \forall v \in H_0^1,$$

which induces the following energy

$$E(v) = \frac{1}{2}(A(\mathbf{p})\nabla v, \nabla v)_{L^2} - (f, v)_{L^2}.$$

For the discretization of  $H_0^1$  we consider classical piecewise linear and continuous finite elements based on a triangulation  $\mathcal{T}_h$  of the domain  $\Omega$ . Let  $V_h$  denote this finite element space. Note that for  $v \in V_h$  the computation of the energy requires the stiffness matrix and the load vector, which can be assembled locally on each triangle in the domain, i.e.,

$$E_T(v) = \frac{1}{2} \int_T A(\mathbf{p})\nabla v \cdot \nabla v \, dx - \int_T f v \, dx.$$

We consider a uniform mesh of size  $h = \sqrt{2} \cdot 2^{-4}$ , which results in 961 degrees of freedom. This means that the output layer of the network contains 961 nodes, while the input layer consists of 3 nodes corresponding to  $(x_0, y_0, r)$ . The network is trained using the ADAM optimizer and  $10^6$  iterations. We use two different widths to explore the impact on accuracy. The training times are reported in Table 1. We deduce that using batches of triangles ( $T = 32$ ) has no effect. The training times are roughly the same as for the full mesh. This is due to the fact that energy computation is done in parallel and the problem is relatively small (the GPU is not maximized).

**Table 1:** Training and inference time for the parameterized problem in section 4.1. Output layer of size 961. Trained on an A100 GPU.

$T$	Dimension	Training time	Inference time
32	$4 \cdot 256$	458 s	1 ms
Full	$4 \cdot 256$	433 s	1 ms
32	$4 \cdot 512$	440 s	1 ms
Full	$4 \cdot 512$	426 s	1 ms

To investigate the error of the method we compute (an approximation of) the expected value of the difference between the output of the network and the finite element approximation in different norms. Given a sample of parameters  $\{\mathbf{p}_i\}_{i=1}^K$  we compute the difference in the energy, the  $L^2$ -norm, and the  $H^1$ -norm, i.e. we compute the relative errors

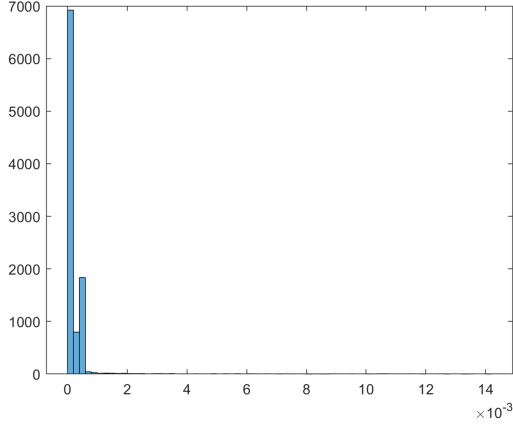
$$\sum_{i=1}^K |E(\mathcal{A}_{h,\theta}(\mathbf{p}_i)) - E(\mathcal{A}_h(\mathbf{p}_i))| / |E(\mathcal{A}_h(\mathbf{p}_i))|, \quad \sum_{i=1}^K \|\mathcal{A}_{h,\theta}(\mathbf{p}_i) - \mathcal{A}_h(\mathbf{p}_i)\|_{L^2} / \|\mathcal{A}_h(\mathbf{p}_i)\|_{L^2},$$

and  $\sum_{i=1}^K \|\mathcal{A}_{h,\theta}(\mathbf{p}_i) - \mathcal{A}_h(\mathbf{p}_i)\|_{H^1} / \|\mathcal{A}_h(\mathbf{p}_i)\|_{H^1}.$

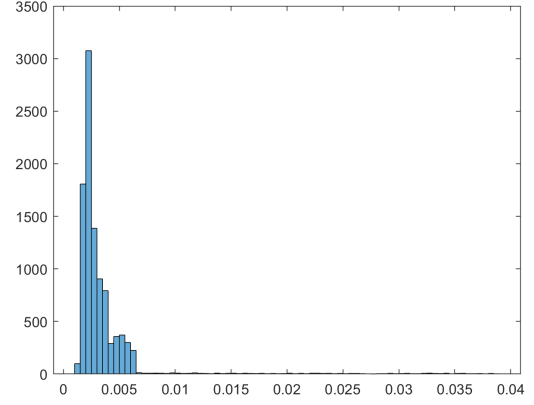
In Table 2 we report mean and standard deviation of these relative errors computed using  $K = 10^4$  samples of the parameter  $\mathbf{p}$ . Corresponding histogram plots are shown in Figure 1 for the network of size  $4 \cdot 256$  and batches using all element sin the mesh. We note that error distribution is small which implies that the network is well trained over the distribution of the parameters. Furthermore, comparing the errors in Table 2 we see that increasing the width of the network improves the approximation properties. We also note that the error naturally increases when using smaller batch sizes of triangles.

**Table 2:** Relative errors for the parameterized problem in section 4.1. Output layer of size 961.

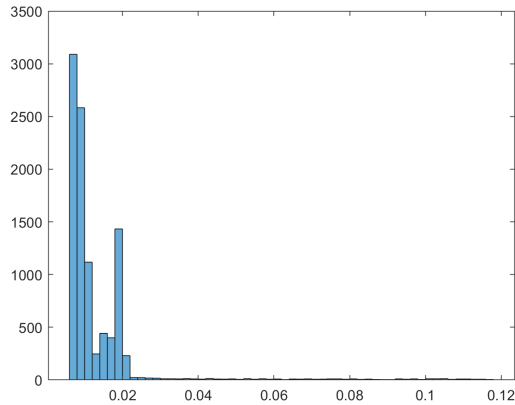
$T$	Dimension	Energy	Std	$L^2$	Std	$H^1$	Std
32	$4 \cdot 256$	0.61%	0.55	2.6%	1.1	6.5%	2.6
Full	$4 \cdot 256$	4.1e-4%	13e-4	0.36%	0.41	1.4%	1.3
32	$4 \cdot 512$	0.45%	0.42	2.4%	1.0	5.7%	2.1
Full	$4 \cdot 512$	2.0e-4%	7.3e-4	0.20%	0.22	0.92%	0.93



(a) Energy



(b)  $L^2$ -norm



(c)  $H^1$ -norm

**Figure 1:** Histogram plots for the different relative errors for a network of size  $4 \cdot 256$  using all elements (full) per batch.

To show a case where batches of triangles does have an effect on the training times, we consider a finer mesh of size  $h = \sqrt{2} \cdot 2^{-7}$  which results in 16129 degrees of freedom

and 32768 triangles. We also increase the width of the neural network to  $4 \cdot 2048$ . In Table 3 the results are reported for batches of size 3277 (10% of the elements) compared to the full mesh. We observe that the training times now are reduced by using a smaller batch of triangles, since the GPU is now maximized and the energy computation can not be completely parallelized in each iteration. The approximation error increases though, since the number of iterations are the same in both cases. We emphasize that for large problems and the choice of GPU model, the batches can have significant impact on the computational times. On a laptop GPU, this could also be crucial to be able to train the network at all.

**Table 3:** A neural network of  $4 \cdot 2048$  hidden layers for the parameterized problem in section 4.1. Output layer of size 16129. Trained on an A100 GPU.

$T$	Training time	Inference time
3277	1720 s	1 ms
Full	1962 s	1 ms

We end this numerical example by noting that the inference time, i.e. the time for one forward pass through the network is very small, around 1 ms in all cases studied. This shows the strength of learning the solution operator. Once trained, the solution for a given parameter is obtained using very little effort.

## 4.2 Gaussian random fields

We consider a Poisson problem with a random coefficient based on a Gaussian random field

$$-\nabla(A(\omega) \cdot \nabla u) = f, \quad \text{in } \Omega, \quad (4.3)$$

$$u = 0, \quad \text{on } \partial\Omega, \quad (4.4)$$

where  $A(\omega)$  is defined as  $\exp a(\omega)$  where  $a(\omega)$  is a Gaussian random field with covariance function given by

$$C(x, y) = \exp\left(-\frac{|x - y|^2}{2L^2}\right)$$

where  $L$  is the correlation length scale. We use a Karhunen-Loève expansion to approximate the field

$$a(x, y, \omega) \approx \mu + \sigma \sum_{i=1}^{N_{KL}} \sqrt{\lambda_i} \phi_i \xi_i(\omega),$$

where  $\mu$  is the constant mean of the field,  $\lambda_i$  and  $\phi_i$  are the eigenvalues and eigenvectors corresponding to the covariance, and  $\xi_i \sim N(0, 1)$  are i.i.d random variables. The number  $N_{KL}$  determines the number of terms in the truncated sum. Similarly to the Poisson problem in Section 4.1, the energy in this setting is given by

$$E(v) = \frac{1}{2}(A(\boldsymbol{\xi})\nabla v, \nabla v)_{L^2} - (f, v)_{L^2},$$



where  $\boldsymbol{\xi}(\omega) = (\xi_1(\omega), \dots, \xi_{N_{KL}}(\omega))$ . The vector  $\boldsymbol{\xi}$  takes different values depending on the realization  $\omega$  and is thus considered the parameter in this case. For the local computations on a triangle we have, c.f. Section 4.1,

$$E_T(v) = \frac{1}{2} \int_T A(\boldsymbol{\xi}) \nabla v \cdot \nabla v \, dx - \int_T f v \, dx.$$

For the numerical experiment we choose  $\mu = 0$ ,  $\sigma = 1$ ,  $L = 0.5$ , and  $N_{KL} = 9$ . For the discretization, we consider a uniform mesh of size  $h = \sqrt{2} \cdot 2^{-5}$ , which results in 3969 degrees of freedom. This means that the output layer of the network contains 3969 nodes, while the input layer consists of 9 nodes corresponding to the length of the vector  $\boldsymbol{\xi}$ . We emphasize that given a realization  $\omega$ , the trained neural network approximates the solution operator by  $u_{h,\theta} = \mathcal{A}_{h,\theta}(\boldsymbol{\xi}(\omega))$ . In Table 4 we report training time for the network. We do not consider batches of triangles in this example, since the number of degrees of freedom is relatively small.

**Table 4:** A neural network of 4 · 512 hidden layers for the Gaussian random field problem in section 4.2. The columns show the total training time and inference time. Trained on an A100 GPU.

T	Training time	Inference time
Full	426 s	1 ms

Similar to first example in Section 4.1 we investigate the error by computing an approximation of the expected value of the difference between the output of the network and the finite element solution. That is, given a sample of parameters  $\{\boldsymbol{\xi}_i\}_{i=1}^K$  we compute the relative errors

$$\sum_{i=1}^K |E(\mathcal{A}_{h,\theta}(\boldsymbol{\xi}_i)) - E(\mathcal{A}_h(\boldsymbol{\xi}_i))| / |E(\mathcal{A}_h(\boldsymbol{\xi}_i))|, \quad \sum_{i=1}^K \|\mathcal{A}_{h,\theta}(\boldsymbol{\xi}_i) - (\mathcal{A}_h(\boldsymbol{\xi}_i))\|_{L^2} / \|(\mathcal{A}_h(\boldsymbol{\xi}_i))\|_{L^2},$$

and  $\sum_{i=1}^K \|\mathcal{A}_{h,\theta}(\boldsymbol{\xi}_i) - (\mathcal{A}_h(\boldsymbol{\xi}_i))\|_{H^1} / \|(\mathcal{A}_h(\boldsymbol{\xi}_i))\|_{H^1}.$

In Table 5 we report mean and standard deviation of these relative errors computed using  $K = 10^4$  samples of the parameter  $\boldsymbol{\xi}$ . Corresponding histogram plots are shown in Figure 2. We note that error distribution is small which implies that the network is well trained over the distribution of the parameters.

**Table 5:** A neural network of 4 · 512 hidden layers for the Gaussian random field problem. The columns show relative errors in different norms using all elements in the mesh. Errors are computed using  $10^4$  samples.

	Energy $E(\cdot)$	$L^2$ -norm	$H^1$ -norm
Mean	3.2e-4%	0.52%	1.3%
Std	4.8e-5	0.29	0.64

For random PDEs we are typically interested in a quantity of interest (QoI), for instance the mean value of the  $L_2$ -norm

$$\mathbb{E}_{\boldsymbol{\xi} \in N(0,1)} [\|u(\boldsymbol{\xi})\|_{L^2}^2].$$

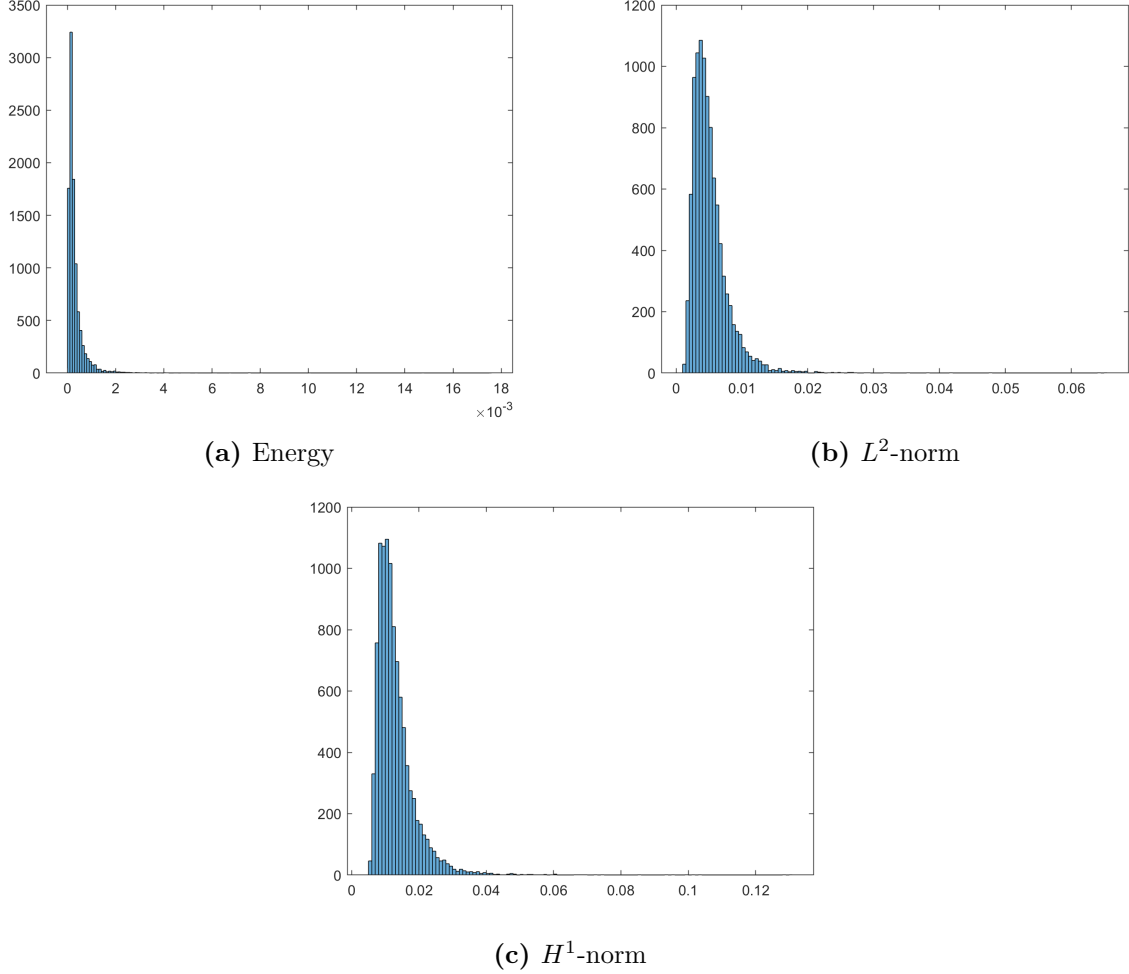


**Figure 2:** Histogram plots for the different relative errors.

or the average point value at some coordinate  $x_0$

$$\mathbb{E}_{\boldsymbol{\xi} \in N(0,1)} [u(x_0, \boldsymbol{\xi})].$$

A classical Monte Carlo approach to approximate the quantity will require many evaluations of the solution operator  $u = \mathcal{A}(\boldsymbol{\xi})$ . For the finite element approximation, this means that we would need to compute an approximation for each realization  $\omega$ . In particular, the stiffness matrix needs to be reassembled for each such realization. However, for the trained neural network, retrieving an approximation for a given realization is a simple forward pass of the network which are typically very fast (around 1 ms). This step is also easily parallelized on the GPU using the JAX framework. To show the advantage of the neural network approach, we compare the computational time for evaluating the quantity of interest using the trained neural network with a finite element approach using the same degrees of freedom. The implementation is done using the FEniCSx library [3]. The GPU computations are performed on the same A100 GPU used for the training and the CPU computations on an Intel(R) Core(TM) i9-11950H 2.60GHz. The results are presented in Table 6-7.

We observe that the neural network clearly outperforms the FEM implementation. In particular when the inference is parallelized on the GPU, but also on a classical CPU when the inferences are done sequentially. This is thus an example of a setting which really

**Table 6:** Computing  $\mathbb{E}_{\boldsymbol{\xi} \in N(0,1)} [\|u(\boldsymbol{\xi})\|_{L^2}^2]$  using  $10^4$  samples.

Method	QoI	GPU (parallel)	CPU (sequential)
NN	0.186	0.21 s	25 s
FEM	0.181	–	79 s

**Table 7:** Computing  $\mathbb{E}_{\boldsymbol{\xi} \in N(0,1)} [u(x_0, \boldsymbol{\xi})]$  for  $x_0 = (0, 0)$  using  $10^4$  samples.

Method	QoI	GPU (parallel)	CPU (sequential)
NN	0.311	0.26 s	20 s
FEM	0.310	–	71 s

shows the potential strength of learning the solution operator using neural networks.

### 4.3 Nonlinear elasticity

A promising application of solution operator networks is to use the output as an initial guess for Newton’s method when solving nonlinear problems, see, e.g., [2, 5, 10]. This is a *complementary* way of using machine learning for PDE solving rather than as a complete solver method, i.e., to consider the operator network’s solution the finished product. Fair criticism towards the latter includes potential loss of accuracy when compared to well-established methods such as FEM. Using the network solution as initial guess for Newton’s method is a way to preserve accuracy and at the same time speed up the iterative process.

Here we consider a nonlinear neo-Hookean elasticity problem: a two dimensional cantilever beam under the influence of a given external force. The external force is defined by two variables: the midpoint of a fixed-length surface interval of application on top of the beam and the vertical magnitude. The solution to the problem is the displacement field over the beam. We generate a structured uniform triangular  $40 \times 2$  mesh of the resting beam and consider standard P1 finite elements. This results in 240 DOFs, since every mesh node ( $41 \cdot 3 = 123$ ) has two DOFs (one for each dimension) and the DOFs of the left-most three nodes are removed since that is where the beam is fixed.

The solution operator we aim to learn is thus the map from the 2 force variables to the 240 finite element DOFs giving the corresponding displacement of the beam. We use a simple MLP architecture that takes 2 input variables (the force variables), has 4 hidden layers of width 256 with ELU activation and one output layer of width 240 (number of DOFs) with no activation. Just as in the previous examples we use the energy functional corresponding to the PDE as the foundation for the loss function.

During training, we pick 32 randomly selected tuples of force variables in each iteration to compute an average loss. The midpoint of the interval of application is sampled uniformly along the beam and the magnitude is sampled from a standard normal distribution. The optimization is performed with the Adam optimizer where we perform  $10^6$  iterations with a decreasing learning rate. The learning rate starts at  $1e-4$  and after every 250k iterations it is decreased by a factor of 0.5.

We consider the specific problem of computing the displacement when the external force is located at the right end of the beam and directed downwards with magnitude 1.0. We perform the Newton iterations with a FEniCS implementation of the problem. All computations are performed on an Apple M1 CPU. Results from using the network

solution and a standard initial guess (the zero function) as input for Newton’s method are presented in Table 8 and Figure 3.

**Table 8:** Computational times for using different initial guesses for Newton’s method.

Initial guess	$E(\text{solution})$	Inference time	Newton solver time	Total time
Network solution	-0.014397	9.4e-5 s	0.015678 s	0.015772 s
Zero function	-0.014397	–	0.022658 s	0.022658 s



(a) Network solution as initial guess.

(b) Zero function as initial guess.

**Figure 3:** Initial guesses for Newton’s method with resulting converged solutions. The converged solution is the same in both cases.

The results in Table 8 and Figure 3 show that using the network solution as initial guess for Newton’s method preserves accuracy while at the same time provides a speed-up compared to using the standard zero function as initial guess. We note that we have not taken the training time of the network into account, so to properly benefit from using the network solution as initial guess a large enough number of problems will have to be solved so that all individual problem gains compensate for the training time.

**Acknowledgement.** This research was supported in part by the Swedish Research Council Grant No. 2021-04925 and Grant No. 2022-03543, and the Swedish Research Programme Essence.

## References

- [1] National academic infrastructure for supercomputing in sweden (naiss), partially funded by the swedish research council through grant agreement no. 2022-06725.
- [2] J. Aghili, E. Franck, R. Hild, V. Michel-Dansac, and V. Vigon. Accelerating the convergence of Newton’s method for nonlinear elliptic PDEs using Fourier neural operators, Mar. 2024. arXiv:2403.03021 [cs, math].
- [3] I. A. Baratta, J. P. Dean, J. S. Dokken, M. Habera, J. S. Hale, C. N. Richardson, M. E. Rognes, M. W. Scroggs, N. Sime, and G. N. Wells. DOLFINx: The next generation FEniCS problem solving environment. Dec. 2023.

- [4] W. E and B. Yu. The deep ritz method: A deep learning-based numerical algorithm for solving variational problems. *Commun. Math. Stat.*, 6.
- [5] J. Huang, H. Wang, and H. Yang. Int-Deep: A deep learning initialized iterative method for nonlinear problems. *Journal of Computational Physics*, 419:109675, Oct. 2020.
- [6] Z. Li, N. Kovachki, K. Azizzadenesheli, B. Liu, K. Bhattacharya, A. Stuart, and A. Anandkumar. Neural operator: Graph kernel network for partial differential equations. *arXiv*, 2003.03485, 2020.
- [7] Z.-Y. Li, N. B. Kovachki, K. Azizzadenesheli, B. Liu, K. Bhattacharya, A. M. Stuart, and A. Anandkumar. Fourier neural operator for parametric partial differential equations. *arXiv*, 2010.08895, 2020.
- [8] L. Lu, P. Jin, G. Pang, Z. Zhang, and G. E. Karniadakis. Learning nonlinear operators via deeponet based on the universal approximation theorem of operators. *Nature Machine Intelligence*, 3:218–229, 2021.
- [9] N. H. Nelsen and A. M. Stuart. The random feature model for input-output maps between banach spaces. *SIAM Journal on Scientific Computing*, 43(5):A3212–A3243, 2021.
- [10] A. Odot, R. Haferssas, and S. Cotin. DeepPhysics: A physics aware deep learning framework for real-time simulation. *International Journal for Numerical Methods in Engineering*, 123(10):2381–2398, 2022. eprint: <https://onlinelibrary.wiley.com/doi/pdf/10.1002/nme.6943>.
- [11] M. Raissi, P. Perdikaris, and G. Karniadakis. Physics-informed neural networks: A deep learning framework for solving forward and inverse problems involving nonlinear partial differential equations. *Journal of Computational Physics*, 378:686–707, 2019.
- [12] M. S. Sacks, S. Motiwale, C. Goodbrake, and W. Zhang. Neural network approaches for soft biological tissue and organ simulations. *Journal of Biomechanical Engineering*, 144(12):121010, 10 2022.
- [13] N. Sharp, C. Romero, A. Jacobson, E. Vouga, P. G. Kry, D. I. Levin, and J. Solomon. Data-free learning of reduced-order kinematics. 2023.

#### Authors' addresses:

Mats G. Larson, <code>mats.larson@umu.se</code>	Mathematics and Mathematical Statistics, Umeå University, Sweden
Carl Lundholm, <code>carl.lundholm@umu.se</code>	Mathematics and Mathematical Statistics, Umeå University, Sweden
Anna Persson, <code>anna.persson@it.uu.se</code>	Information Technology-Scientific Computing, Uppsala University, Sweden